USCT data challenge 2019

C. Boehm[1], T. Hopp[2], and N. Ruiter[2]

[1] *ETH Zurich, Switzerland, E-mail: christian.boehm@erdw.ethz.ch*
[2] *Karlsruhe Institute of Technology, Germany*

Abstract

Recent years have witnessed the active development of scanning systems and reconstruction algorithms for ultrasound computed tomography (USCT) with applications to breast imaging for early cancer detection. Despite these advances in hardware and software development, we encounter the need for reference data to develop, test and compare different imaging methods. With the goals of encouraging scientific exchange and collaborations, providing benchmarks of reconstruction algorithms, and standardizing USCT data formats, we have released open-source data sets of simulated waveforms that mimic measurements of a USCT scanning aperture using numerical breast phantoms. This is part of ongoing efforts centered around the USCT platform for data exchange and collaboration [1, 2].

Keywords: ultrasound computer tomography, numerical modelling, data challenge

1   Introduction

Within the past decade, substantial progress in the development and design of USCT systems has been made, and several systems have readily provided first clinical results [3, 4, 5]. Simultaneously, a wide range of image reconstruction methods using both transmission and reflection data has been developed. Overviews of different modelling and inversion techniques can be found in [6] and [7]. One of the main challenges is to find good trade-offs between the quality of the image, on the one hand, and the time-to-solution, on the other hand. Popular reconstruction methods include ray-based time-of-flight inversion [8, 9, 10], reflection imaging using synthetic aperture focusing techniques [11] and reverse time migration [12], Born modelling [13, 14], as well as waveform tomography and full-waveform inversion in time and frequency domain [15, 16, 17, 18, 19, 20, 21, 22].

While this list is far from being complete, the variety of imaging and reconstruction algorithms readily stresses the need for suitable reference data to benchmark and compare different methods. To meet the demand for freely available data sets within the USCT research
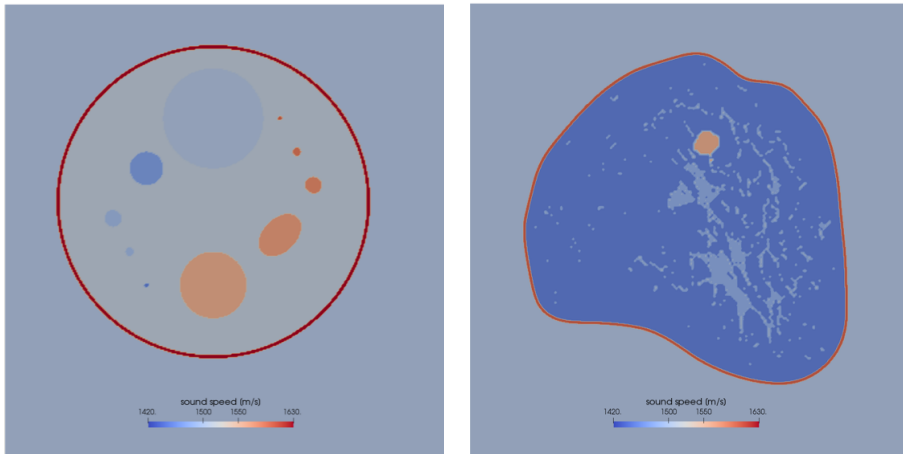
Figure 1: Sound speed map of the analytical **(left)** and the segmented breast phantom **(right)** used in the simulations.

community, a digital platform hosting several data sets has been initiated. In the initial phase this included raw data donated by three different USCT systems [1, 2]. In the course of this new data challenge, we added simulated A-scans using numerical phantoms that enable researchers to compare and benchmark different reconstruction algorithms with a ground truth.

The long term goals of this initiative are (1) to build up an open-source reference USCT data base that is freely available for the entire community, (2) to enable reproducible comparisons of image reconstruction algorithms and USCT systems, (3) to establish user friendly interfaces, standards and data formats between different USCT apertures, reconstruction algorithms, software and data formats, and (4) to identify properties of systems, experimental setups, data, and algorithms towards optimal images.

In the rest of the paper we briefly summarize the specification of the numerical phantoms used in this data challenge, comment on the scanning aperture and simulation setup, and propose a flexible data format for USCT scans.

2   Numerical phantoms

This data challenge comprises waveform data for two different numerical phantoms. Figure 1 shows the sound speed map of both phantoms. In addition, data generated in a homogeneous medium mimicking an empty water tank with a constant sound speed of 1500 m/s and a density of 1000 kg / m^3 is provided for calibration purposes.

Ellipse	Center (x, y) [mm]	Axes (x, y) [mm]	θ [°]	c [m/s]	ρ [kg / m^3]
a	(0, 0)	(47, 47)	0	1650	1150
b	(0, 0)	(46, 46)	0	1510	1040
c	(0, -25)	(10, 10)	0	1560	1070
d	(0, 25)	(15, 15)	0	1500	990
e	(20, -10)	(5, 7.5)	45	1570	1080
f	(30, 5)	(2.5, 2.5)	0	1580	1090
g	(20, 25)	(0.625, 0.625)	0	1600	1150
h	(-20, 10)	(5, 5)	0	1470	980
i	(-30, -5)	(2.5, 2.5)	0	1490	1000
j	(-25, -15)	(1.25, 1.25)	0	1490	1100
j	(-20, -25)	(0.625, 0.625)	0	1450	960

Table 1: The geometric parameters used for creating the analytic phantom as well as the values for sound speed c and density ρ. The order is important and later added shapes overwrite the previous values.

Tissue	c [m/s]	ρ [kg / m^3]
water	1500	1000
fat	1450	980
glandular tissue	1480	1020
skin	1600	1060
muscle	1580	1080
irregular cancer	1550	1070
lobular cancer	1560	1010
cyst	1500	1000
fibroadenoma	1530	1080

Table 2: Values of sound speed c and density ρ for different tissues labelled in the segmented phantom.

2.1 Analytic shapes

The first breast phantom is a superposition of spheres and ellipses with different sizes and constant material properties, and has a diameter of 94 mm. Table 1 provides the full description of all shapes.

2.2 Segmented MRI data

The second phantom is a 2D coronal slice of segmented MRI data of a human breast. The discrete values assigned to the different tissue labels are given in Table 2. As exact tissue parameters are still controversially discussed, we empirically selected values which are in the range of the values reported across the literature [23]. The resolution of the original MRI is fairly coarse with a voxel size of 0.68359 mm and 311×316 pixels in the coronal plane. This yields an irregular pattern, which is primarily visible in the skin. At high frequencies, this stair-casing effect can lead to significant distortion and spurious reflections as shown in Figure 2. To mitigate this effect, we smooth the skin layer in a preprocessing step.
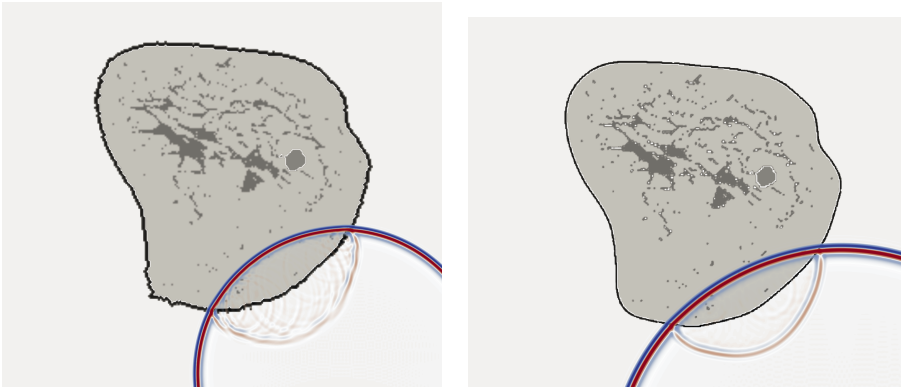

Figure 2: Snapshots of the pressure field. Using the raw MRI data to obtain the speed map leads to signifcant distortion at the water-skin interface (**left**). This unphysical effect can be mitigated by smoothing the sound speed model in a preprocessing step (**right**).

3 Aperture and simulated data

We simulate the time-domain acoustic wave equation parameterized by a heterogeneous density ρ and sound speed c:

$$\frac{1}{\rho(\mathbf{x})c(\mathbf{x})^2}\partial_{tt}\phi(\mathbf{x},t) - \nabla \cdot \frac{1}{\rho(\mathbf{x})}\nabla\phi(\mathbf{x},t) = s(t)\delta(\mathbf{x}-\mathbf{x}_s), \tag{1}$$
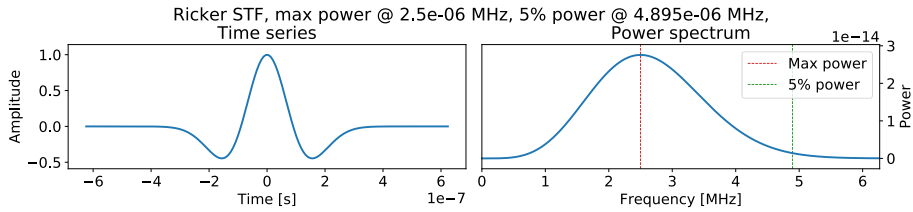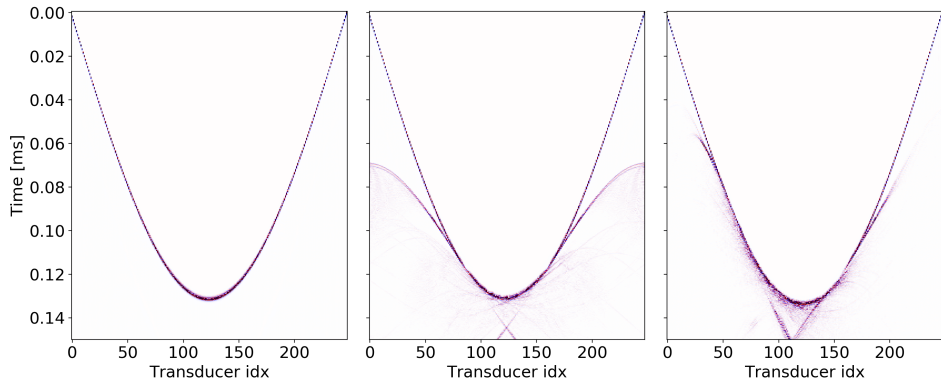
Figure 3: Source wavelet in time domain and its power spectral density.

Figure 4: Signal gathers for synthetic waveforms computed in water **(left)**, the analyitc phantom **(middle)**, and the segmented phantom **(right)**. The colorscale is centered around zero and clips large amplitudes to highlight reflected and refracted waveforms after the first arrival.

with homogenuous initial conditions

$$\phi(\mathbf{x},0) = \partial_t \phi(\mathbf{x},0) = 0, \qquad (2)$$

where ϕ denotes the time- and space-dependent wavefield and s is the source-time function of an omni-directional point source emitting at location $\mathbf{x}_s$. The source time function is a Ricker wavelet, centered around time zero. The dominant frequency for the 2D data is 2.5 MHz, and the frequency cutoff of 5% of the power spectrum is close to 5 MHz, cf. Fig. 3. The 2D simulations use an aperture with 249 transducers aligned on a ring with a radius of 99 mm. The simulation domain uses a box extended along both coordinate axis and with absorbing boundary conditions imposed on all side walls. The duration of the simulation spans 0.150635 ms, and the data are sampled with a time increment of 9.4 ns. Fig. 4 shows collected A-scans for a single emitter in a homogenuous medium and both numerical phantoms. Reflections from the skin and the stronger sounds speed anomalies can be distinguished in the data of the analytical phantom. This is not the case for the segmented phantom All simulations were carried out using the spectral-element method [24].
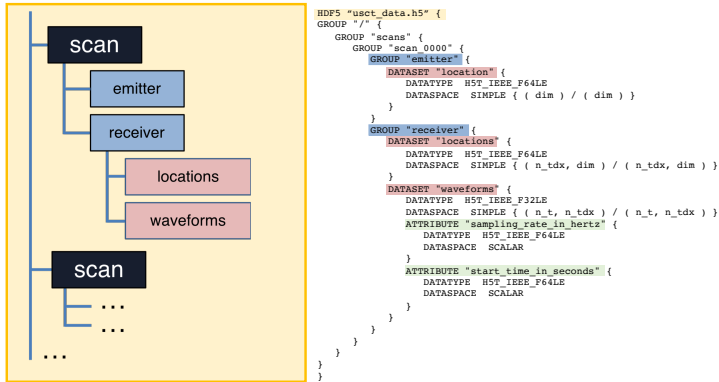
Figure 5: Sketch of the container structure within **(left)** and how this translates into groups and datasets in the hdf5 file **(right)**. Note that additional meta data can easily be stored as attributes or auxiliary datasets. Data types and data set dimensions are dynamic.

4 Data format

To the best of our knowledge, no standardized file format to easily store, process and transfer USCT raw data has emerged from the community yet. As part of releasing data for this challenge, we propose a flexible data format based on HDF5 [25], a widespread, open-source library for storing scientific data. HDF5 has built-in support for compression, chunking, check summing and variable floating point precision. Internally, the file is organized in a container-like structure similar to a filesystem tree. This permits storing waveform data and meta information together in a single file. Furthermore, data from multiple scans can easily be combined or split into several files.

Figure 5 provides a high-level view on the proposed container structure. All information can be accessed individually, which permits lazy loading and batch-wise operations if memory is scarce. Wrappers for reading and writing file contents are currently available for Python, Matlab, C++. We also provide a validation tool to ensure compliance with the file format definition.

5 Conclusions

The aim of this work is to provide freely available simulated USCT data to test and benchmark different imaging algorithms. These simulated data of numerical phantoms follow the previous USCT data challenge that provided measurements from different scanning systems.

The data and a small collection of software tools are available open-source, and we hope to also include inversion and imaging algorithms in the future. We will continue to maintain and extend this platform, and we welcome active participation and feedback. This will contribute to the overarching goals of this initiative, which are to facilitate research on early breast cancer detection, improve imaging algorithms and scanning apertures, and to foster scientific collaborations.

Acknowledgement

References

[1] N. V. Ruiter, M. Zapf, T. Hopp, H. Gemmeke, and K. W. A. van Dongen, "USCT data challenge," in *Medical Imaging 2017: Ultrasonic Imaging and Tomography* (N. Duric and B. Heyde, eds.), vol. 10139, pp. 412 – 419, International Society for Optics and Photonics, SPIE, 2017.

[2] N. V. Ruiter, M. Zapf, T. Hopp, H. Gemmeke, K. W. A. van Dongen, J. Camacho, J. L. Herraiz, M. P. Liva, and J. M. Udías, "USCT reference data base: conclusions from the first SPIE USCT data challenge and future directions," in *Medical Imaging 2018: Ultrasonic Imaging and Tomography* (N. Duric and B. C. Byram, eds.), vol. 10580, pp. 170 – 176, International Society for Optics and Photonics, SPIE, 2018.

[3] M. André, J. Wiskin, and D. Borup, "Clinical results with ultrasound computed tomography of the breast," in *Quantitative Ultrasound in Soft Tissues* (J. Mamou and M. L. Oelze, eds.), pp. 395–432, Dordrecht: Springer Netherlands, 2013.

[4] N. Duric, P. Littrup, C. Li, O. Roy, S. Schmidt, X. Cheng, J. Seamans, A. Wallen, and L. Bey-Knight, "Breast imaging with SoftVue: initial clinical evaluation," in *Medical Imaging 2014: Ultrasonic Imaging and Tomography* (J. G. Bosch and M. M. Doyley, eds.), vol. 9040, pp. 208 – 215, International Society for Optics and Photonics, SPIE, 2014.

[5] H. Gemmeke, T. Hopp, M. Zapf, C. Kaiser, and N. V. Ruiter, "3d ultrasound computer tomography: Hardware setup, reconstruction methods and first clinical results," *Nuclear Instruments and Methods in Physics Research Section A: Accelerators, Spectrometers, Detectors and Associated Equipment*, vol. 873, pp. 59 – 65, 2017. Imaging 2016.

[6] R. J. Lavarello and A. J. Hesford, "Methods for forward and inverse scattering in ultrasound tomography," in *Quantitative Ultrasound in Soft Tissues* (J. Mamou and M. L. Oelze, eds.), pp. 345–394, Dordrecht: Springer Netherlands, 2013.

[7] N. Ozmen, R. Dapp, M. Zapf, H. Gemmeke, N. V. Ruiter, and K. W. A. van Dongen, "Comparing different ultrasound imaging methods for breast cancer detection," *IEEE Transactions on Ultrasonics, Ferroelectrics, and Frequency Control*, vol. 62, pp. 637–646, April 2015.

[8] S. Li, M. Jackowski, D. P. Dione, T. Varslot, L. H. Staib, and K. Mueller, "Refraction corrected transmission ultrasound computed tomography for application in breast imaging," *Medical Physics*, vol. 37, no. 5, pp. 2233–2246, 2010.

[9] M. Pérez-Liva, J. L. Herraiz, L. Medina-Valdés, J. Camacho, C. Fritsch, B. E. Treeby, and J. M. Udías, "Regularization of image reconstruction in ultrasound computed tomography," in *2015 IEEE Nuclear Science Symposium and Medical Imaging Conference (NSS/MIC)*, pp. 1–3, Oct 2015.

[10] T. Hopp, M. Zapf, H. Gemmeke, and N. V. Ruiter, "Experimental evaluation of straight ray and bent ray phase aberration correction for USCT SAFT imaging," in *Medical Imaging 2018: Ultrasonic Imaging and Tomography* (N. Duric and B. C. Byram, eds.), vol. 10580, pp. 136 – 148, International Society for Optics and Photonics, SPIE, 2018.

[11] T. Hopp, F. Zuch, M. Zapf, H. Gemmeke, and N. V. Ruiter, "Experimental analysis of ray-based sound speed reconstruction algorithms for phase aberration corrected USCT SAFT imaging," in *Medical Imaging 2019: Ultrasonic Imaging and Tomography* (B. C. Byram and N. V. Ruiter, eds.), vol. 10955, pp. 128 – 138, International Society for Optics and Photonics, SPIE, 2019.

[12] O. Roy, M. A. H. Zuberi, R. G. Pratt, and N. Duric, "Ultrasound breast imaging using frequency domain reverse time migration," in *Medical Imaging 2016: Ultrasonic Imaging and Tomography* (N. Duric and B. Heyde, eds.), vol. 9790, pp. 84 – 92, International Society for Optics and Photonics, SPIE, 2016.

[13] J. Wiskin, D. Borup, S. Johnson, and M. Berggren, "Non-linear inverse scattering: High resolution quantitative breast tissue tomography," *The Journal of the Acoustical Society of America*, vol. 131, no. 5, pp. 3802–3813, 2012.

[14] N. K. Martiartu, C. Boehm, and A. Fichtner, "3d wave-equation-based finite-frequency tomography for ultrasound computed tomography," 2019.

[15] R. G. Pratt, L. Huang, N. Duric, and P. Littrup, "Sound-speed and attenuation imaging of breast tissue using waveform tomography of transmission ultrasound data," *Proc. SPIE*, vol. 6510, p. 65104S, 2007.

[16] G. Sandhu, C. Li, O. Roy, S. Schmidt, and N. Duric, "Frequency domain ultrasound waveform tomography: breast imaging using a ring transducer," *Physics in medicine and biology*, vol. 60, no. 14, p. 5381, 2015.

[17] A. Goncharsky, S. Y. Romanov, and S. Y. Seryozhnikov, "A computer simulation study of soft tissue characterization using low-frequancy ultrasonic tomography," *Ultrasonics*, vol. 67, pp. 136–150, 2016.

[18] T. P. Matthews, K. Wang, C. Li, N. Duric, and M. A. Anastasio, "Regularized dual averaging image reconstruction for full-wave ultrasound computed tomography," *IEEE Transactions on Ultrasonics, Ferroelectrics, and Frequency Control*, vol. 64, no. 5, pp. 811–825, 2017.

[19] M. Perez-Liva, J. L. Herraiz, J. M. Udias, E. Miller, B. T. Cox, and B. E. Treeby, "Time domain reconstruction of sound speed and attenuation in ultrasound computed tomography using full wave inversion," *The Journal of the Acoustical Society of America*, vol. 141, no. 3, pp. 1595–1604, 2017.

[20] A. Ihrig and G. Schmitz, "Accelerating nonlinear speed of sound reconstructions using a randomized block kaczmarz algorithm," in *2018 IEEE International Ultrasonics Symposium (IUS)*, pp. 1–9, Oct 2018.

[21] C. Boehm, N. K. Martiartu, N. Vinard, I. J. Balic, and A. Fichtner, "Time-domain spectral-element ultrasound waveform tomography using a stochastic quasi-Newton method," in *Medical Imaging 2018: Ultrasonic Imaging and Tomography* (N. Duric and B. C. Byram, eds.), vol. 10580, pp. 92 – 100, International Society for Optics and Photonics, SPIE, 2018.

[22] O. C. Agudo, L. Guasch, P. Huthwaite, and M. Warner, "3D imaging of the breast using full-waveform inversion," in *Proceedings of the International Workshop on Medical Ultrasound Tomography: 1.-3. Nov. 2017*, p. 99, KIT Scientific Publishing, 2018.

[23] P.A. Hasgall, F. Di Gennaro, C. Baumgartner, E. Neufeld, B. Lloyd, M.C. Gosselin, D. Payne, A. Klingenböck, N. Kuster, "IT'IS Database for thermal and electromagnetic parameters of biological tissues," Version 4.0," 2018.

[24] M. Afanasiev, C. Boehm, M. van Driel, L. Krischer, M. Rietmann, D. A. May, M. G. Knepley, and A. Fichtner, "Modular and flexible spectral-element waveform modelling in two and three dimensions," *Geophysical Journal International*, vol. 216, no. 3, pp. 1675–1692, 2019.

[25] The HDF Group, "Hierarchical Data Format, version 5," 1997-2017. http://www.hdfgroup.org/HDF5/.